

Dependence of the Minority-Carrier Lifetime on the Stoichiometry of CdTe Using Time-Resolved Photoluminescence and First-Principles Calculations

Jie Ma, Darius Kuciauskas, David Albin, Raghu Bhattacharya, Matthew Reese, Teresa Barnes, Jian V. Li, Timothy Gessert, and Su-Huai Wei

National Renewable Energy Laboratory, Golden, Colorado 80401, USA

(Received 4 February 2013; published 7 August 2013)

CdTe is one of the most promising materials for thin-film solar cells. However, further improvement of its performance is hindered by its relatively short minority-carrier lifetime. Combining theoretical calculations and experimental measurements, we find that for both intrinsic CdTe and CdTe solar cell devices, longer minority-carrier lifetimes can be achieved under Cd-rich conditions, in contrast to the previous belief that Te-rich conditions are more beneficial. First-principles calculations suggest that the dominant recombination centers limiting the minority-carrier lifetime are the Te antisite and Te interstitial. Therefore, we propose that to optimize the solar cell performance, extrinsic *p*-type doping (e.g., *N*, *P*, or As substitution on Te sites) in CdTe under Cd-rich conditions should be a good approach to simultaneously increase both the minority-carrier lifetime and hole concentration.

DOI: [10.1103/PhysRevLett.111.067402](https://doi.org/10.1103/PhysRevLett.111.067402)

PACS numbers: 78.47.jd, 61.72.J-, 71.15.Mb, 88.40.jm

CdTe is one of the most promising photovoltaic absorbers for thin-film solar cell devices, due to its near-optimum band gap (~ 1.5 eV), high absorption coefficient, and low cost. Its theoretical efficiency for converting terrestrial sunlight can be as high as $\sim 29\%$ [1]. A critical problem for CdTe solar cells is that the open-circuit voltage (V_{OC}) and fill factor (FF) remain lower than expected for a 1.5 eV band gap material. The experimental efficiency has so far only reached 19.6% [2]. One of the main reasons for the low V_{OC} and FF is the relatively short minority-carrier lifetime. Unless the minority-carrier lifetime can be increased, the open-circuit voltage will still be low. Furthermore, although we may gain improved open-circuit voltage by increasing net acceptor doping, the current density and FF will both decrease if the minority-carrier lifetime remains unchanged, because the photon-generated carriers cannot be collected efficiently [3,4]. The main process that limits the minority-carrier lifetime in CdTe is defect-mediated recombination. According to the Shockley-Read-Hall model [5,6], the most efficient recombination centers are defects with deep levels in the middle of the band gap. In order to improve the minority-carrier lifetime, the recombination process has to be suppressed, and therefore the concentrations of deep-level defects have to be reduced. Determining the main deep-level defects in CdTe and controlling their concentrations are crucial issues for making high-efficiency CdTe solar cells.

It is well known that in semiconductors the stoichiometry determines defect concentrations, which affect material properties, including free-carrier concentration, mobility, optical absorption or emission, and minority-carrier lifetime [7,8]. However, there are surprisingly few reports discussing the effect of stoichiometry on the minority-carrier lifetime in CdTe. A previous theoretical model based on local density approximation (LDA) suggests

that the Te vacancy (V_{Te}) could be the main deep-level defect in CdTe [9]. Therefore, reducing the Te vacancy concentration through Te-rich conditions could minimize the recombination and thus improve the minority-carrier lifetime. Many experimental groups rely on the assumption that higher CdTe growth temperatures would yield better device performance, because high growth temperatures should make CdTe more Te rich based on the phase diagram [10]. However, because LDA underestimates the band gap, the defect-level predictions, especially for anion vacancies, may need reexamination. Moreover, a recent experiment [11] showed that when extra Te was introduced through the back surface of CdTe devices, which should make the material more Te rich and passivate the Te vacancies, both the minority-carrier lifetime and solar cell efficiency dropped significantly. This experiment suggests that the Te vacancy may not be the most important detrimental defect in CdTe solar cells.

In this Letter, combining advanced theoretical calculations and experimental measurements, we show that longer minority-carrier lifetimes are actually achieved under Cd-rich conditions. Time-resolved photoluminescence (TRPL) is employed to measure the minority-carrier lifetime in intrinsic CdTe. While traditional one-photon excitation (1PE) measurements could be limited by fast surface recombination, the two-photon excitation (2PE) TRPL technique allows for the determination of minority-carrier lifetimes. We find that the minority-carrier lifetimes are significantly greater in Cd-rich CdTe (~ 20 ns) compared to Te-rich CdTe (~ 3 ns). We also find the same behavior in CdTe solar cell devices: the minority-carrier lifetime increases as the CdTe layer is more Cd rich. First-principles calculations using hybrid functional [12] are employed to calculate the intrinsic defects in CdTe. We find that the Te vacancy is a shallow donor rather than a

deep-level defect. The most important deep-level defects limiting minority-carrier lifetimes are the Te interstitial and Te antisite. The calculated results are in agreement with our experimental observations that Cd-rich CdTe has longer minority-carrier lifetimes.

Large-grained (approximately 1 mm grain size) polycrystalline CdTe samples (polycrystals) were supplied by Redlen Technologies, Inc. (British Columbia, Canada), with the specification of either 40 ppm excess Cd or Te. Our inductively coupled plasma mass spectrometry (ICP MS) measurements indicated that the Cd:Te ratio for the Te-rich sample was 0.99 ± 0.01 and that for the Cd-rich sample was 1.01 ± 0.01 . The trend of this variation in stoichiometry was verified consistently in several samples. The single-phase, homogeneity region for CdTe is capable of supporting a maximum excess of only 4×10^{-3} at. % Cd or 13×10^{-3} at. % Te [10]. Though ICP MS measurements do not approach this resolution, they do provide a qualitative verification.

TRPL was used to study the excess-carrier recombination at room temperature. Excitation was provided by a regeneratively amplified Yb:KGW laser system and an optical parametric amplifier (OPA). The laser repetition rate was 1.1 MHz, and the pulse length was 0.3 ps. The OPA wavelength was set at 630 nm (1.97 eV) for 1PE and 1170 nm (1.06 eV) for 2PE. The average laser power used in the measurements was 2 mW and 20 mW for 1PE and 2PE, respectively. Excitation pulses were delivered and photoluminescence (PL) signals were collected using an optical fiber and a dichroic beam splitter [13]. Because of the propagation in the optical fiber, the laser pulse length was increased to 0.45 ps. No attempt was made to compensate for this temporal broadening. The estimated excitation spot size was $250 \mu\text{m}$ and $50 \mu\text{m}$ in 1PE and 2PE measurements, respectively. PL signals were recorded using a 10 nm bandwidth interference filter and Si avalanche photodiode. Time-correlated single photon counting was used to acquire TRPL decays.

Figure 1 shows the TRPL decays measured with 1PE and 2PE. The 1PE TRPL decays [Fig. 1(a)] for the Cd-rich and Te-rich samples are almost identical. Because CdTe has a high absorption coefficient (characteristic absorption depth $1/\alpha_{630\text{nm}} = 0.22 \mu\text{m}$), the 1PE laser pulses are mostly absorbed in the sample surface region and the TRPL decays are dominated by fast surface recombination. For analysis, we employed an exponential fitting model with deconvolution of the instrumental response [13]. Around 90% of the decay has an excess-carrier lifetime of 0.2 ± 0.1 ns. Similar fast TRPL decays were previously reported [14,15]. Because of the fast surface recombination, possible minority-carrier lifetime differences between the Cd-rich and Te-rich CdTe cannot be established by 1PE TRPL.

Now we consider the 2PE TRPL data in Fig. 1(b). The low-intensity laser pulses with photon energy less than the band gap will propagate through the material with no absorption.

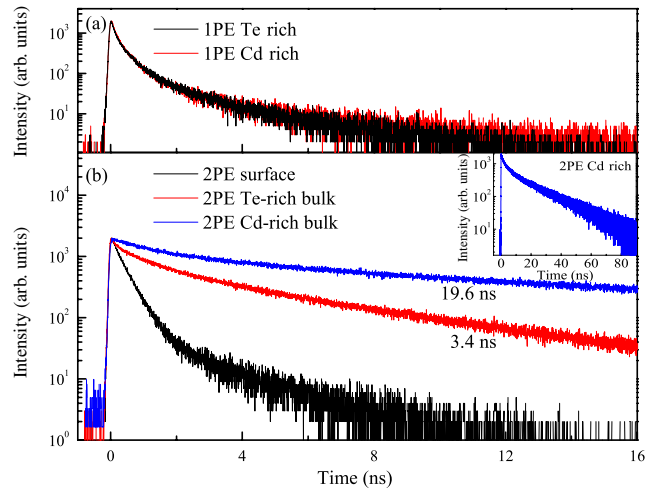


FIG. 1 (color online). The 1PE (a) and 2PE (b) TRPL decays. The 1PE data are identical for Cd-rich and Te-rich samples. The 2PE data show that the minority-carrier lifetime in the Cd-rich sample (19.6 ns) is nearly six times longer than that in the Te-rich sample (3.4 ns). The inset in (b) shows the full TRPL decay of the Cd-rich sample. When the focus of the 2PE laser beam is close to the surface [black curve in (b)], the 2PE decay reproduces the 1PE results, which confirms that the fast decay in 1PE measurements is due to fast surface recombination.

However, if the laser beam is focused by a lens, the nonlinear 2PE may occur at the focal point of the laser beam [16]. By translating the CdTe sample with a micrometer-controlled stage, the laser beam focus can be moved from the surface into the bulk, such that the recombination rate in the bulk can be determined. When the laser beam is focused close to the sample surface, the TRPL decay [black curve in Fig. 1(b)] is very similar to the 1PE data, which confirms that 1PE TRPL decays reflect fast surface recombination. When the focus of the laser beam is moved from the surface to the bulk, we observe a gradual reduction of the amplitude of the fast decay component. To measure the recombination rate in the bulk, we focus the laser beam ~ 0.5 mm below the surface, and fit TRPL decays with an exponential function [17,18]. As shown in Fig. 1(b), the 2PE TRPL decays for both Cd-rich and Te-rich samples [curves labeled with 19.6 and 3.4 ns in Fig. 1(b)] have substantially longer lifetimes. Repeated measurements of different sample areas indicate a lifetime of 3.4 ± 1.0 ns for the Te-rich samples and 19.6 ± 3.3 ns for the Cd-rich samples. Variation of the 2PE laser power in the range of 10–50 mW shows that lifetimes remained essentially unchanged. This result suggests that 2PE measurements correspond to low-injection conditions and that the TRPL lifetimes indicate bulk minority-carrier lifetimes in Te-rich and Cd-rich samples. From the 2PE TRPL measurements, it is clearly observed that the minority-carrier lifetime in Cd-rich CdTe is nearly six times longer than that in Te-rich CdTe.

Next, we consider the minority-carrier lifetime in polycrystalline CdTe thin-film solar cell devices. These cells

incorporate common processing steps (necessary to attain cell efficiency $>12\%$) that introduce Cl and Cu impurities. The cell fabrication details were described in previous work [19]. Several cells were prepared in this work, with the primary difference being the temperature at which the CdTe layer was deposited. According to the phase diagram, CdTe deposited at a high temperature tends to be more Te rich and CdTe deposited at a low temperature tends to be more Cd rich [10]. This stoichiometry trend was again confirmed by ICP MS. The corresponding Cd:Te ratios of the CdTe films grown at 484 °C and 625 °C were 1.00 ± 0.01 and 0.98 ± 0.01 , respectively.

After fabrication, the recombination rates in these cells were measured by 1PE TRPL. Details of the TRPL data analysis to determine the minority-carrier lifetime in solar cell devices were recently described [13,20]. The measured minority-carrier lifetimes are shown in Fig. 2. At a growth temperature of 625 °C, where the CdTe layer is more Te rich, the minority-carrier lifetime is only 1–2 ns; at a growth temperature of 484 °C, where the CdTe layer is more Cd rich, the minority-carrier lifetime can increase to nearly 10 ns. It is clear that as the growth temperature decreases, CdTe becomes more Cd rich and the minority-carrier lifetime increases. These results corroborate what was observed in intrinsic CdTe and suggest that despite further processing steps that introduce Cl and Cu doping, the benefits of Cd-rich stoichiometry remain for improving the minority-carrier lifetime. The averaged efficiencies of the solar cells made at each temperatures are 12.37% (484 °C), 12.62% (550 °C), and 11.21% (625 °C), and the averaged V_{OC} are 0.83 (484 °C), 0.81 (550 °C), and 0.78 V (625 °C), respectively. These parameters generally improve as the minority-carrier lifetime increases. The

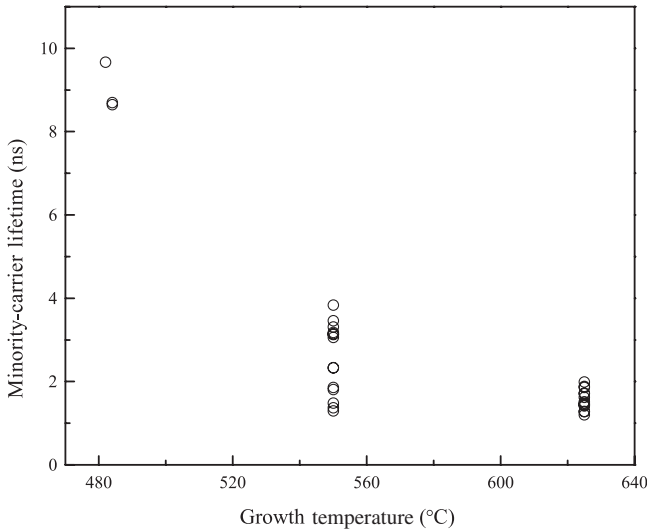


FIG. 2. The minority-carrier lifetimes of polycrystalline CdTe thin-film solar cell devices as a function of CdTe growth temperature. As the growth temperature decreases, CdTe becomes more Cd rich, and the minority-carrier lifetime increases.

improvement is small because the hole concentration is low in Cd-rich CdTe [3].

Our calculations were based on (generalized) Kohn-Sham theory [21] as implemented in VASP code [22]. Because LDA [21] underestimates band gaps [23,24], we employed the Heyd-Scuseria-Ernzerhof 2006 (HSE06) hybrid functional [12]. The hybrid functional generally shows improvements in structural, electronic, and defect properties in semiconductors [25–32]. The projector augmented wave pseudopotentials [33] were employed and the valence wave functions were expanded in a plane-wave basis with an energy cutoff of 300 eV. The Brillouin zone integration was sampled with $2 \times 2 \times 2$ k -point mesh and a 64-atom cubic supercell was employed. The calculated band gap of CdTe is 1.41 eV.

The formation energy of a defect α in charge state q is defined as

$$\Delta H_f(\alpha, q) = \Delta E(\alpha, q) + \sum_i n_i \mu_i + q E_F, \quad (1)$$

where $\Delta E(\alpha, q) = E(\alpha, q) - E(\text{host}) + \sum_i n_i E(i) + q \epsilon_{\text{VBM}}(\text{host})$. $E(\alpha, q)$ is the energy for a supercell containing the relaxed defect α in charge state q ; $E(\text{host})$ is the energy of the host in the same supercell without the defect; $\epsilon_{\text{VBM}}(\text{host})$ is the energy of the valence band maximum (VBM) of the host; E_F is the Fermi energy referenced to the VBM; μ_i is the chemical potential of constituent i referenced to elemental solid or gas with energy $E(i)$; and n_i is the number of atoms transferred from the supercell to reservoirs in forming the defect. Under equilibrium conditions, the chemical potentials fulfill $\mu_{\text{Cd}} \leq 0$, $\mu_{\text{Te}} \leq 0$, and $\mu_{\text{Cd}} + \mu_{\text{Te}} = \Delta H_f(\text{CdTe})$ with $\Delta H_f(\text{CdTe})$ as the formation energy of the CdTe solid. To overcome the finite supercell size issue, the defect transition energy level is calculated with the mixed k -point scheme [8]:

$$\epsilon_\alpha(q/q') = [\epsilon_D^\Gamma - \epsilon_{\text{VBM}}(\text{host})] + [E(\alpha, q) - E(\alpha, q')] - (q' - q) \epsilon_D^k / (q' - q), \quad (2)$$

where ϵ_D^Γ and ϵ_D^k are the energies of defect band at Γ point and special k points (weight averaged), respectively. The computational details have been discussed in previous publications [8].

The calculated formation energies of the intrinsic defects at the most stable charge state are displayed in Fig. 3. Comparing the HSE06 data to the previous LDA data [9,34,35], we find that the most significant difference is the Te vacancy. It is a shallow donor in HSE06 calculations, but in LDA calculations it is a mid-gap defect [9]. Figure 4 shows the single-electron level (Kohn-Sham eigenvalue) of the Te vacancy within HSE06 and LDA calculations. The single-electron levels of the neutral state within HSE06 and LDA calculations are 0.08 eV above and 0.74 eV below the VBM, and those of the 2+ charged state are pushed up to 2.48 eV and 1.54 eV above the VBM due to the large atomic displacement, respectively. The LDA

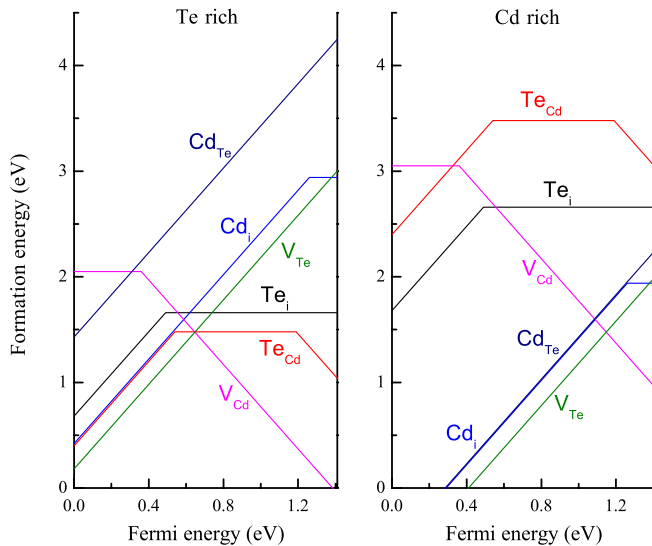


FIG. 3 (color online). The HSE06 formation energies of the intrinsic defects at the most stable charge state as a function of the Fermi energy, under the Te-rich condition ($\mu_{\text{Te}} = 0$) (left), and Cd-rich condition ($\mu_{\text{Cd}} = 0$) (right).

levels are lower in energy than the HSE06 levels. Within the HSE06 calculation, the average of these two levels is 0.13 eV below the conduction band minimum (CBM), which is an adequate estimate of the defect transition energy level. Within the LDA, the average is 0.4 eV above the VBM. Because the calculated LDA band gap of CdTe is 0.63 eV, the band gap must be corrected to get a reasonable transition energy level. Empirical corrections are often employed to shift the band-edge states. However, how to shift the defect level correspondingly usually varies from

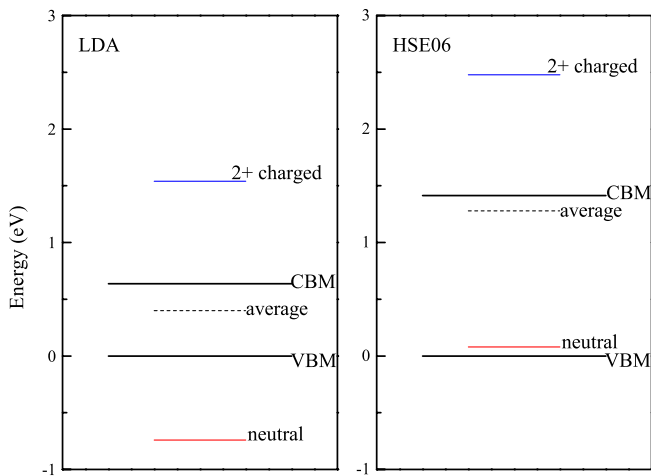


FIG. 4 (color online). The single-electron levels of the Te vacancy within LDA (left) and HSE06 (right). The red, blue, and dashed black lines indicate the single-electron levels of the neutral defect, the 2+ charged defect, and their average, respectively. The solid black lines indicate the positions of the VBM and CBM of CdTe. The energy of the VBM is set to zero.

one group to another [7,36–42]. If we do not shift the defect level up with the CBM, we can reproduce the previous LDA results where the Te vacancy is a deep-level defect [9,34], but if we shift up the defect level rigidly with the CBM, we can get a similar result to HSE06, where it is a shallow donor. It is clear that the difference in the positions of the single-electron levels is the reason for the difference in transition energy levels. The HSE06 calculations suggest that the defect level of the Te vacancy is mostly derived from the CBM, and thus should be shifted up following the CBM. This is consistent with our finding that the defect level of the Te vacancy and the CBM in CdTe have similar *s*-like wave functions.

In previous LDA calculations [9], the Te vacancy is a deep-level defect. According to the SRH model [5,6], it is an effective recombination center. Thus, a longer minority-carrier lifetime should be achieved under Te-rich conditions, which differs from our experimental results. In the HSE06 calculations, the Te vacancy is not a deep-level defect and should not affect the minority-carrier lifetime. Instead, the Te interstitial and Te antisite, which are more energetically favorable under Te-rich conditions, are the main deep-level defects limiting the minority-carrier lifetime. Therefore, the HSE06 results suggest that a longer minority-carrier lifetime should be achieved under Cd-rich conditions, which is in agreement with our experiments on both intrinsic CdTe and polycrystalline CdTe solar cell devices. Our deep-level transient spectroscopy measurements (see the Supplemental Material [43]) show that as CdTe becomes more Cd rich, the concentrations of near mid-gap defects decrease, which is also consistent with our HSE06 results.

In conclusion, we have studied the minority-carrier lifetime in CdTe both experimentally and theoretically. The TRPL measurements suggest that both intrinsic CdTe and CdTe thin-film solar cell devices have longer minority-carrier lifetimes under Cd-rich conditions. The HSE06 results are in agreement with the experiments and suggest that the main recombination centers limiting the minority-carrier lifetime are the Te antisite and Te interstitial. In reality, because it is believed that Te-rich conditions are beneficial for *p*-type doping (i.e., V_{Cd} , Cu_{Cd} , etc.), a balance that optimizes both the minority-carrier lifetime and hole density is required. Generally, under cation-rich conditions, anion-site dopants are energetically favorable. Therefore, to improve device performance, growing CdTe under Cd-rich conditions and doping with extrinsic *p*-type dopants, such as *N*, *P*, or *As* substitution on Te sites, should be beneficial.

The authors are grateful to Glenn Bindley and Bob Redden at Redlen Technologies for providing the CdTe materials with controlled stoichiometry used in this work, and to Pat Dippo for photoluminescence measurements. The authors further acknowledge the support of the U.S. Department of Energy under Contract No. DE-AC36-08-GO28308 with the National Renewable Energy Laboratory.

- [1] C.H. Henry, *J. Appl. Phys.* **51**, 4494 (1980).
- [2] M.A. Green, K. Emery, Y. Hishikawa, W. Warta, and E.D. Dunlop, *Prog. Photovoltaics* **21**, 827 (2013).
- [3] J. Sites and J. Pan, *Thin Solid Films* **515**, 6099 (2007).
- [4] A. Kanevce and T.A. Gessert, *IEEE J. Photovoltaics* **1**, 99 (2011).
- [5] W. Shockley and W.T. Read, *Phys. Rev.* **87**, 835 (1952).
- [6] R.N. Hall, *Phys. Rev.* **87**, 387 (1952).
- [7] C.G. Van de Walle and J. Neugebauer, *J. Appl. Phys.* **95**, 3851 (2004).
- [8] S.-H. Wei, *Comput. Mater. Sci.* **30**, 337 (2004).
- [9] S.-H. Wei and S.B. Zhang, *Phys. Rev. B* **66**, 155211 (2002).
- [10] J.H. Greenberg, *J. Cryst. Growth* **161**, 1 (1996).
- [11] T.A. Gessert *et al.*, *Thin Solid Films* **535**, 237 (2013).
- [12] A.V. Krukau, O.A. Vydrov, A.F. Izmaylov, and G.E. Scuseria, *J. Chem. Phys.* **125**, 224106 (2006).
- [13] D. Kuciauskas, A. Kanevce, J.M. Burst, J.N. Duenow, R. Dhere, D.S. Albin, D.H. Levi, and R.K. Ahrenkiel, *IEEE J. Photovoltaics* **PP**, 1 (2013).
- [14] W.K. Metzger, D. Albin, M.J. Romero, P. Dippo, and M. Young, *J. Appl. Phys.* **99**, 103703 (2006).
- [15] C.J. Bridge, P. Dawson, P.D. Buckle, and M.E. Ozsan, *J. Appl. Phys.* **88**, 6451 (2000).
- [16] S.J. Bepko, *Phys. Rev. B* **12**, 669 (1975).
- [17] R.K. Ahrenkiel, N. Call, S.W. Johnston, and W.K. Metzger, *Solar Energy Mater. Sol. Cells* **94**, 2197 (2010).
- [18] S. Jursenas, S. Miasojedovas, A. Zukauskas, B. Lucznik, I. Grzegory, and T. Suski, *Appl. Phys. Lett.* **89**, 172119 (2006).
- [19] D.H. Rose, F.S. Hasoon, R.G. Dhere, D.S. Albin, R.M. Ribelin, X.S. Li, Y. Mahathongdy, T.A. Gessert, and P. Sheldon, *Prog. Photovoltaics* **7**, 331 (1999).
- [20] A. Kanevce, D.H. Levi, and D. Kuciauskas, *Prog. Photovoltaics* (in press).
- [21] W. Kohn and L.J. Sham, *Phys. Rev.* **140**, A1133 (1965).
- [22] G. Kresse and J. Furthmuller, *Phys. Rev. B* **54**, 11169 (1996).
- [23] J.P. Perdew and M. Levy, *Phys. Rev. Lett.* **51**, 1884 (1983).
- [24] L.J. Sham and M. Schluter, *Phys. Rev. Lett.* **51**, 1888 (1983).
- [25] J. Paier, M. Marsman, K. Hummer, G. Kresse, I. C. Gerber, and J.G. Angyan, *J. Chem. Phys.* **124**, 154709 (2006).
- [26] P. Broqvist and A. Pasquarello, *Appl. Phys. Lett.* **89**, 262904 (2006).
- [27] D. Munoz Ramo, J.L. Gavartin, A.L. Shluger, and G. Bersuker, *Phys. Rev. B* **75**, 205336 (2007).
- [28] A. Alkauskas, P. Broqvist, and A. Pasquarello, *Phys. Rev. Lett.* **101**, 046405 (2008).
- [29] F. Oba, A. Togo, I. Tanaka, J. Paier, and G. Kresse, *Phys. Rev. B* **77**, 245202 (2008).
- [30] M.-H. Du and S.B. Zhang, *Phys. Rev. B* **80**, 115217 (2009).
- [31] A. Janotti, J.B. Varley, P. Rinke, N. Umezawa, G. Kresse, and C.G. Van de Walle, *Phys. Rev. B* **81**, 085212 (2010).
- [32] M.-H. Du and K. Biswas, *Phys. Rev. Lett.* **106**, 115502 (2011).
- [33] G. Kresse and D. Joubert, *Phys. Rev. B* **59**, 1758 (1999).
- [34] M.-H. Du, H. Takenaka, and D.J. Singh, *J. Appl. Phys.* **104**, 093521 (2008).
- [35] K. Biswas and M.-H. Du, *New J. Phys.* **14**, 063020 (2012).
- [36] S.B. Zhang, *J. Phys. Condens. Matter* **14**, R881 (2002).
- [37] S. Lany and A. Zunger, *Phys. Rev. B* **78**, 235104 (2008).
- [38] A. Janotti and C.G. Van de Walle, *Phys. Rev. B* **76**, 165202 (2007).
- [39] S.B. Zhang, S.-H. Wei, and A. Zunger, *Phys. Rev. B* **63**, 075205 (2001).
- [40] P. Agoston, K. Albe, R.M. Nieminen, and M.J. Puska, *Phys. Rev. Lett.* **103**, 245501 (2009).
- [41] S. Lany and A. Zunger, *Phys. Rev. Lett.* **93**, 156404 (2004).
- [42] S. Lany and A. Zunger, *Phys. Rev. B* **72**, 035215 (2005).
- [43] See Supplemental Material at <http://link.aps.org/supplemental/10.1103/PhysRevLett.111.067402> for the description of our deep-level transient spectroscopy measurements.